Automated light-based mapping of motor cortex by photoactivation of channelrhodopsin-2 transgenic mice

Oliver G S Ayling[1,2,5], Thomas C Harrison[1,2,5], Jamie D Boyd[3,5], Alexander Goroshkov[3] & Timothy H Murphy[1,2,4]

Traditionally, mapping the motor cortex requires electrodes to stimulate the brain and define motor output pathways. Although effective, electrode-based methods are labor-intensive, potentially damaging to the cortex and can have off-target effects. As an alternative method of motor mapping, we photostimulated transgenic mice expressing the light-sensitive ion channel channelrhodopsin-2 in predominantly layer-5 output cortical neurons. We report that optical stimulation of these neurons *in vivo* using a stage scanning laser system resulted in muscle excitation within 10–20 ms, which can be recorded using implanted electromyogram electrodes or by a noninvasive motion sensor. This approach allowed us to make highly reproducible automated maps of the mouse forelimb and hindlimb motor cortex much faster than with previous methods. We anticipate that the approach will facilitate the study of changes in the location and properties of motor maps after skilled training or damage to the nervous system.

The motor cortex was the first region of the brain to be mapped and to have an overt function attributed to it[1]. Motor mapping technologies have been refined in the intervening years and now include intracortical microstimulation (ICMS)[2] and surface stimulation with electrode arrays[3]. The advent of transcranial magnetic stimulation has made noninvasive motor mapping feasible in humans[4]. Each of these techniques has unique advantages and limitations. Transcranial magnetic stimulation is noninvasive but has poor spatial resolution. Electrode-based brain stimulation methods have common disadvantages: the inability to selectively target neuronal subtypes, indiscriminate activation of axons of passage and damage when impalements are made.

Recently it has become possible to stimulate neurons using light, either by uncaging neurotransmitters[5,6] or by directly activating light-sensitive channels[7,8]. Channelrhodopsin-2 (ChR2) is a light-activated nonselective cation channel isolated from the green alga *Chlamydomonas reinhardtii*[9], which when expressed in neurons can transduce light energy into neural activity[10]. Here we present hardware and software for light-based mapping (LBM) of motor cortex output from anesthetized mice expressing ChR2 (ref .11). High-resolution motor maps are generated quickly, reliably and accurately in mice using a stage scanning system and fixed laser. We offer investigators a tool with greatly improved speed and precision to interrogate the motor cortex and address questions about sensorimotor processing both in the normal brain and after training, injury or disease.

RESULTS

Automated mapping of motor cortex using laser light

For automated ChR2-based motor mapping we chose a relatively collimated 473 nm laser targeted through a simple microscope (**Fig. 1a**). To check the beam profile as it passes through brain tissue, we directed the beam into the cortical surface of a fixed mouse brain section (**Fig. 1b**). The beam width (measured using a monochrome camera) was 170 ± 3.7 μm at the cortical surface and 640 ± 220 μm at a depth of 250 μm ($n = 7$ measurements; all values are reported as mean ± s.d.; **Fig. 1c**). Examination of light intensity at different depths indicated that beam width decreased exponentially with a decay constant of ~450 μm.

For LBM, we moved the mouse relative to the laser using a fast scanning stage (13 mm s^{-1})[12]. We moved the stage in random order to each of the predefined stimulation locations superimposed on the cortical map (**Fig. 1a**), and delivered a flash of laser light to each point while collecting an electromyogram (EMG) and a cortical electroencephalogram (EEG). We selected the intensity and duration of photostimulation based on their ability to elicit a suprathreshold EMG response.

Photostimulation elicited homogeneous cortical excitation

After verifying that the stage scanning laser system was accurate in positioning, we tested its ability to evoke local excitation of the cortex by performing a craniectomy and then placing surface EEG electrodes made of silver wire in the four corners of the craniectomy. We mapped EEG responses over areas of up to 20 mm^2 divided into activation sites of ~0.09 mm^2 (300 μm spacing) and found that photostimulation excited all regions of the exposed cortex (**Fig. 2a–c**). Homogeneity of cortical excitation ensured that

[1]Kinsmen Laboratory, Department of Psychiatry, 2255 Wesbrook Mall, [2]Brain Research Center, 2211 Wesbrook Mall, [3]In Vivo Imaging Centre, 2350 Health Sciences Mall, [4]Department of Cellular and Physiological Sciences, University of British Columbia, 2255 Wesbrook Mall, Vancouver, V6T 1Z3, Canada. [5]These authors contributed equally to this work. Correspondence should be addressed to T.H.M. (thmurphy@interchange.ubc.ca).

RECEIVED 23 SEPTEMBER 2008; ACCEPTED 9 JANUARY 2009; PUBLISHED ONLINE 15 FEBRUARY 2009; DOI:10.1038/NMETH.1303

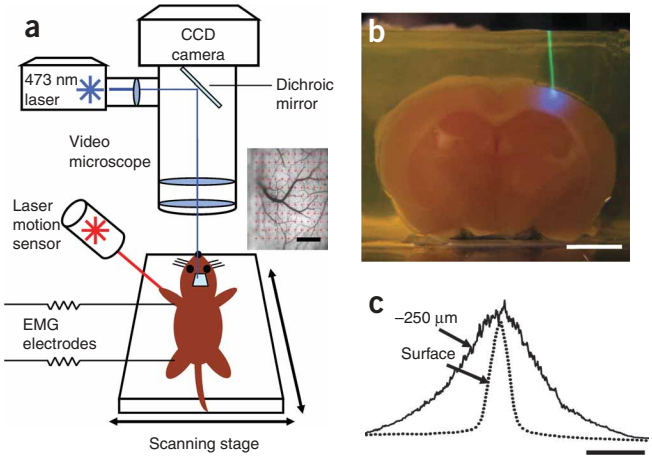

Figure 1 | Automated LBM of the mouse motor cortex. (**a**) Experimental setup. Anesthetized mice were placed on a scanning stage and an array of cortical points (inset) was stimulated by a 473 nm collimated laser beam directed through a video microscope objective. Motor output was detected by EMG electrodes in forelimb and hindlimb muscles, and by a laser motion sensor fixed to the stage. (**b**) Photograph of a stimulation laser targeted at a coronal slice of fixed brain tissue embedded in carboxyfluorescein-containing agarose. (**c**) Intensity profile of the illuminated area as the beam passes through fluorescent agarose above the surface of the brain and 250 μm under the cortical surface (peaks were normalized for comparison). Images used for analysis were acquired using a high-resolution monochromatic camera. Scale bars, 1 mm (**a**), 2 mm (**b**) and 400 μm (**c**).

differences in motor maps reflect local motor output circuitry and not the distribution of ChR2 responsiveness.

In evaluating EEG recordings, we found that photostimulation as short as 1–5 ms evoked a response. These brief light flashes produced cortical depolarizations that were significantly longer than the stimulus duration (31.4 ± 5.4 ms, $P < 0.0001$, $n = 15$ trials in four mice, unpaired *t*-test; **Fig. 2d**). We also found that targeting the laser at the exposed EEG electrode caused a large photoelectric artifact that was different in kinetics from the results of cortical tissue excitation and was restricted to periods when the laser was activated. As expected, wild-type mice lacking ChR2 showed no response to photostimulation ($n = 6$) but did show the photoelectric artifact (**Supplementary Fig. 1** online).

To confirm the expression of ChR2-YFP protein reported by the developers of the mouse[11] and the distributor (Jackson Labs), we performed a histological examination of ChR2-YFP fluorescence in a subset of mice ($n = 3$; **Supplementary Fig. 2** online). We corroborated the homogeneous distribution of ChR2-YFP fusion protein throughout the sensorimotor cortex and its restriction to tufted layer-5 neurons as originally reported, and this was consistent with other *Thy1* promoter–driven mouse lines[11,13]. In two mice examined by confocal microscopy we saw no labeling of neuronal cell bodies in more superficial layers (**Supplementary Fig. 2**).

Mapping light-evoked muscle potentials in ChR2 mice

By implanting silver EMG electrodes in the triceps brachii (extensor) and extensor carpi radialis brevis muscles of the forelimb, and the biceps femoris (flexor) and vastus lateralis (extensor) of the hindlimb, we established the parameters of LBM necessary to evoke contralateral EMG responses. We assessed the effect of light intensity (40–600 mW mm^{-2}) and stimulus duration (1–35 ms), and found that these ranges of intensity and duration were sufficient to produce a motor response (**Fig. 2d**). Photoactivation of areas 170 μm in diameter reliably evoked a motor cortex EEG response and a delayed EMG response in contralateral forelimb and contralateral hindlimb muscles. We did not study smaller photoactivation areas because the arbors of layer-5 neurons are at least 300 μm across, and we would not expect any increase in detail with reduced photoactivation areas.

We assigned processed EMG responses a grayscale value on a linear scale from black (zero) to white (maximum response) to form a pixel-based map, typically created with grids of stimulation points using 300 μm spacing (**Fig. 3a–d** and **Supplementary Methods** online). Given some scattering of blue light by tissue[14], this spatial frequency should efficiently excite the cortex between each of the points and is consistent with photoactivation areas used in previous brain-slice and *in vivo* work[11,14].

Photostimulation in the center of motor maps yielded muscle excitation after a delay from the photostimulation onset of 10.8 ± 1.0 ms for contralateral forelimb and 19.4 ± 1.0 ms for contralateral hindlimb EMG ($n = 4$ mice). Analysis of the relationship between cortical EEG depolarization and evoked EMG signals (**Fig. 2d**) revealed the latency between cortical excitation and muscle excitation. As expected, optically evoked EMG responses exhibited latencies comparable to those of EMG responses produced by direct electrode-based stimulation of motor cortex in mice and other animals (**Fig. 3e,f**)[15]. In ICMS experiments, the latency of ICMS-evoked EMG responses was 11.1 ± 1.1 ms for contralateral forelimb and 19.5 ± 0.9 ms for contralateral hindlimb ($n = 4$ mice), consistent with values from photostimulation experiments. Cortical regions from which LBM evoked larger EMG responses tended to also produce responses with shorter latencies (**Supplementary**

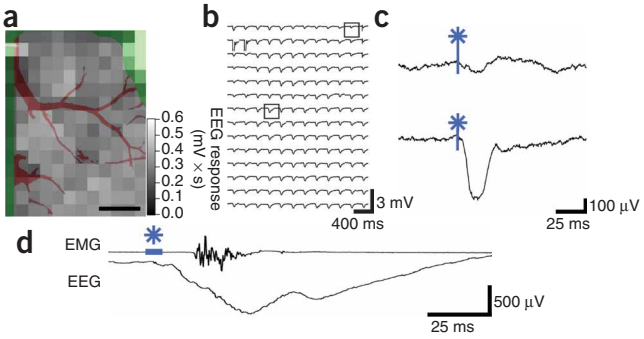

Figure 2 | ChR2-mediated EEG responses can be elicited from all regions of the exposed cortex. (**a**) Mean EEG responses evoked when the laser stimulated that cortical location from four electrodes at the cortical surface. EEG amplitudes were normalized to the maximum value (within each electrode), and then the mean values from all four electrodes were averaged. Lighter colors signify a larger response. The linear scale was set to emphasize variations in cortical response. At points of stimulation where the cortical surface was obstructed by blood vessels or bone (colored red and green, respectively), responses were diminished or absent. Scale bar, 1 mm. (**b**) Raw EEG traces from a single electrode. (**c**) Traces (boxed in **b**) showing a representative EEG response evoked by stimulation over bone (top) and of exposed cortex (bottom). Optical stimulation began at the point marked by the asterisk. (**d**) The relative time courses of ChR2-evoked EEG and EMG responses are shown after a single 5 ms pulse of 160 mW mm^{-2} laser light (blue bar). Note the prolonged EEG depolarization relative to stimulus duration.

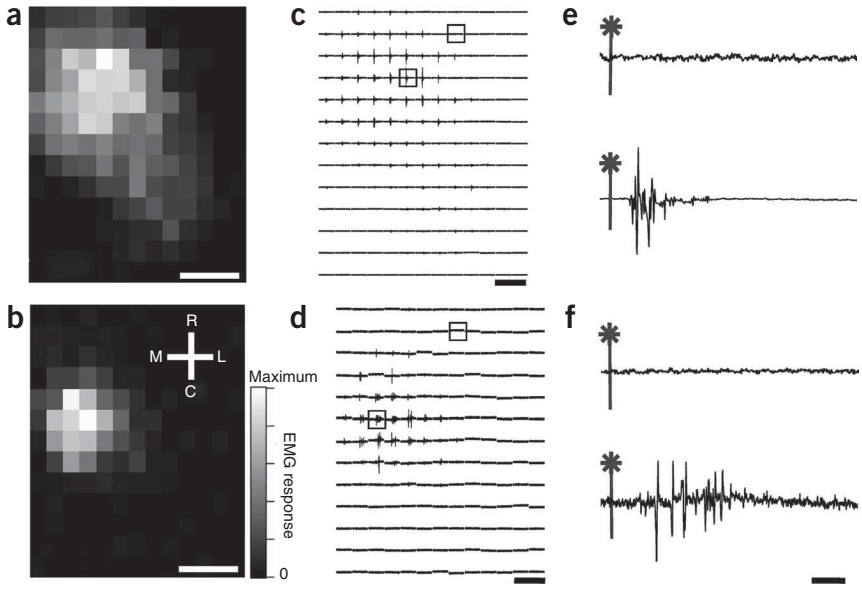

Figure 3 | High-resolution optically stimulated motor maps. (**a**,**b**) Forelimb triceps brachii (**a**) and hindlimb biceps femoris (**b**) motor maps created with 320 μm spacing between laser stimulation points (single 15 ms pulses at 160 mW mm^{-2}). Each map is the average of three repetitions. Absolute grayscale values are not equivalent for **a** and **b**. M, medial; L, lateral; R, rostral; and C, caudal. (**c**,**d**) One repetition of raw EMG traces for forelimb (**c**) and hindlimb (**d**), with individual traces arranged according to the cortical locations from which they were evoked by photostimulation. (**e**,**f**) Boxes in **c** and **d** identify expanded forelimb (**e**) and hindlimb (**f**) EMG traces with an asterisk indicating the onset of laser stimulation. Responses to optical stimulation of points outside the motor maps (top traces) and inside the motor maps (bottom traces) are shown. Scale bars, 1 mm (**a**,**b**), 200 ms (**c**,**d**) and 20 ms (**e**,**f**).

Fig. 3 online). In a mouse on which we performed both ICMS and LBM (**Fig. 4**), the positions and sizes of motor maps were generally in agreement. In this combined ICMS and LBM experiment we performed 26 penetrations to map the motor cortex, completing the ICMS map in approximately 1 h. In the same amount of time, we could map more than 3,000 points using LBM.

Given that layer-5 neurons make corticospinal projections, it is likely that LBM does not require intracortical excitatory synaptic activity to stimulate muscles. Application of α-amino-3-hydroxyl-5-methyl-4-isoxazole-propionate (AMPA) and *N*-methyl-D-aspartic acid (NMDA)-type glutamate receptor antagonists (**Supplementary Methods** and **Supplementary Fig. 4** online) directly to the sensorimotor cortex at concentrations and durations previously shown to block sensory signals[16] suggested that LBM activates corticofugal projections directly and not antagonist-sensitive circuitous intracortical routes of motor activation.

To estimate the area of cortex activated by light pulses, we examined intrinsic optical signals (IOS) in response to 100 ms trains of light pulses and found them to spread over 1,012 ± 316 μm (n = 4 mice, measured at full width at half-maximal amplitude; **Supplementary Methods** and **Supplementary Fig. 5** online) consistent with the extent of light scattering observed at a depth of 250 μm (**Fig. 1c**). In comparison, we observed ICMS electrode activation widths of 690 ± 102 μm (n = 3 mice), indicating that LBM activates an area only moderately larger than ICMS (~2.2-fold larger). The IOS response area within a contour plot drawn at 75% of the peak laser activation was considerably smaller (0.22 mm^2 or about 0.5 mm in diameter; **Supplementary Fig. 5**). These measurements suggest relative differences between ICMS and LBM activation areas; however, the use of IOS activation area to determine exactly what fraction of output neurons are activated with a single light pulse may be complicated by potential non-linearity associated with IOS measurements and by uncertainty of the relevant firing thresholds.

Regarding phototoxicity, we observed no consistent decrease in the amplitudes of evoked EEGs or EMGs during an experiment and no gross histological evidence of damage. In two mice involved in particularly long experiments, EMG amplitude showed no measurable reduction after >100 stimulus repetitions made over the same areas (**Supplementary Fig. 6** online). By making a sealed chronic cranial window and using a noninvasive laser–based measurement device[17] we found in two preliminary experiments that similar forelimb movement maps could be evoked in sessions 7–10 d apart, indicating that LBM does not lead to slowly developing toxicity (**Supplementary Fig. 7** online). The laser motion sensor was more sensitive to paw movements than visual assessment and provided data on an absolute scale that agreed with EMG-based maps (**Supplementary Fig. 8** online).

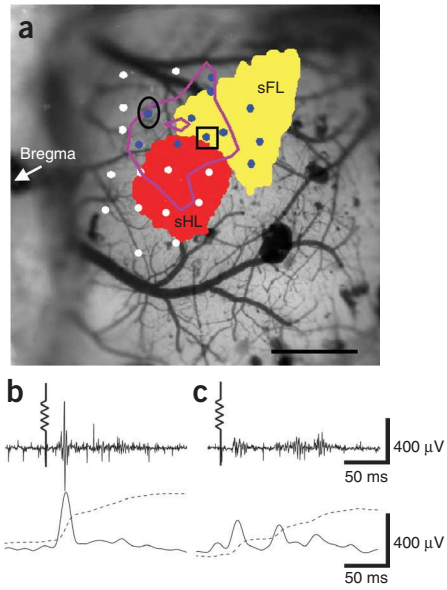

Figure 4 | ICMS and LBM motor maps obtained from the same ChR2-positive mouse. (**a**) Points of electrode-based ICMS trains are displayed in blue (forelimb movement) and white (no forelimb movement). Purple contour lines represent the ChR2-derived LBM forelimb motor map created with single 20 ms, 160 mW mm^{-2} laser pulses (90% and 50% of peak response). IOS sensory maps are displayed in yellow for sensory forelimb sFL and red for sensory hindlimb sHL. Scale bar, 1 mm. (**b**,**c**) Raw EMG (top), full wave rectified response (bottom, solid line) and integrated response (bottom, dashed line) for the ICMS point of stimulation marked in **a** by the square (**b**) and the oval (**c**). Electrode symbol indicates stimulus onset.

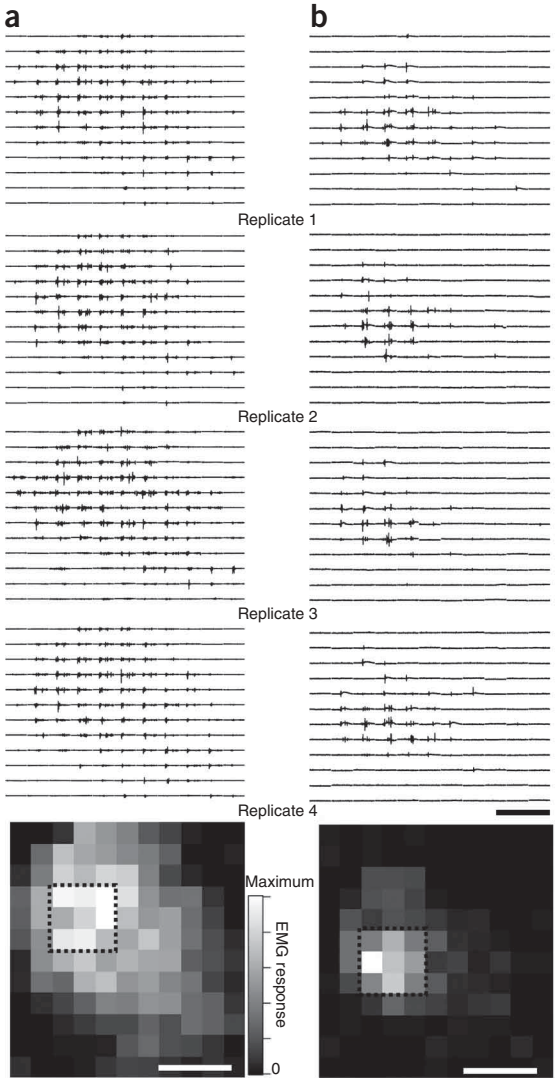

Figure 5 | Motor maps are stable and repeatable. (**a**,**b**) Four consecutive replicates (numbered) of forelimb (**a**) and hindlimb (**b**) EMGs in response to laser stimulation using 10 ms, 160 mW mm^{-2} blue-light pulses. The resulting four motor maps were generated in ~100 s per repetition. In each array, individual EMG traces (200 ms long) are plotted according to the stimulation position from which they were evoked. These spatial relationships are preserved in the pixel-based maps of response amplitude. The mean response within a 9-pixel region of interest at the center of each map (as defined by two-dimensional Gaussian fit) was 38.4 ± 10.0 mV × ms for contralateral hindlimb and 848 ± 74.3 mV × ms for contralateral forelimb. Stimulation was performed with 300 μm spacing between points, and each pixel represents a cortical area of 0.09 mm^2. Scale bars, 500 ms (top) and 1 mm (bottom).

Fine motor map structure

Repeated LBM maps from the same mouse indicated that spatial heterogeneity in EMG amplitude was not due to noise or poor sampling but reflected the underlying properties of the motor representations (**Fig. 5**). To examine limb representations on a finer scale, we compared the size and center positions of two different muscles within a motor map of a single limb by one-way ANOVA ($P = 0.0007$) and Tukey post-hoc tests. Contralateral forelimb extensor muscle maps were similar in size when thresholded at 50% of maximal amplitude (**Supplementary Methods**): carpi radialis brevis and triceps brachii muscle maps were 1.65 ± 0.61 mm^2 ($n = 9$ mice) and 1.60 ± 0.67 mm^2 ($n = 7$), respectively ($P > 0.05$). The same was true for the hindlimb biceps femoris flexor and vastus lateralis extensor maps (0.71 ± 0.30 mm^2 ($n = 5$) and 0.61 ± 0.28 mm^2 ($n = 7$), respectively; $P > 0.05$). Both contralateral forelimb maps were significantly larger than either of the contralateral hindlimb maps ($P < 0.05$), which is consistent with epidural array-based mapping studies in the rat[3]. Similar to map area, differences in motor map position were significant only when comparisons were made between contralateral forelimb and contralateral hindlimb, and not between muscles within the same limb. Forelimb muscle representations had a mean center point that was separated from the center of the combined hindlimb map by an average distance of 0.46 ± 0.25 mm ($P = 0.0005$, $n = 9$ mice, one-sample two-tailed t-test). Our map analysis suggests that muscles working together to control a body part were represented in very similar regions of motor cortex, whereas muscles in different appendages overlapped less. In eight mice we defined map coordinates with reference to bregma (**Supplementary Table 1** online).

We examined the spatial relationships between sensory and motor representations of contralateral forelimb and contralateral hindlimb ($n = 3$ mice; **Fig. 6**). Approximately 50% of contralateral forelimb and contralateral hindlimb motor maps overlapped with sensory cortex (**Supplementary Table 2** online). Although there is some uncertainty about the motor map edge position (to within 500 μm), the motor and sensory map center positions should be more precise. The distances between the centers of the forelimb motor and sensory maps were 1,217 ± 669 μm, and centers of hindlimb motor and sensory maps were 540 ± 454 μm apart.

DISCUSSION

Given that electrode impalements require several minutes each, we estimate that LBM is two orders of magnitude faster than electrode-based techniques. We anticipate that such an approach will be useful for determining changes in motor map structure before and after stroke or spinal cord injury[18–20].

Although we performed mostly acute experiments, LBM is ideally suited to longitudinal experiments and can be performed multiple times on the same mouse through a chronic craniectomy[21]

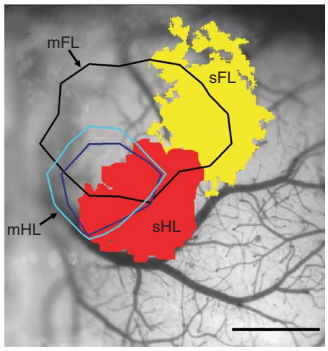

Figure 6 | Motor and sensory cortical limb representations. Sensory forelimb (sFL) and sensory hindlimb (sHL) representations were visualized using IOS imaging (thresholded at 50% of maximal response). Contour lines at 50% of peak response are shown for the extensor carpi radialis forelimb muscle (mFL) and the hindlimb biceps femoris (mHL) and vastus lateralis (dark blue) motor maps derived from single 5 ms, 330 mW mm^{-2} laser pulses. Scale bar, 1 mm.

or possibly a thinned-skull preparation[22]. Notably, we observed some activation through thinned bone at the edge of the craniectomy (**Supplementary Fig. 7**). Repeated ICMS (on the same rat) has been conducted in the past[23,24], but the likelihood of damaging the brain makes LBM a better choice for longitudinal studies of reorganization following experimental manipulations.

Other advantages of LBM over penetrating electrodes are related to sampling. With LBM, stimulation points can be arrayed in a perfect grid, ensuring a more uniform sampling of the cortex than is possible with ICMS. We found that the presence of large blood vessels did not completely block the photoactivation of ChR2, and that motor maps could be obtained even in areas occupied by large vessels, something that would not be possible with ICMS (**Fig. 2a**).

LBM appears to detect motor representations selectively as the resulting forelimb and hindlimb motor maps were located medial to the respective sensory maps (**Fig. 6**) in the approximate location expected for the mouse motor cortex[17,25] and in agreement with observations in rats[3]. Although the size and center of the forelimb and hindlimb motor representations were different, the two territories exhibited considerable spatial overlap. Possibly motor map overlap between limbs could reflect activation at off-target sites resulting from light scattering or spatial overlap between axonal or dendritic arbors of forelimb and hindlimb motor cortex. Alternatively, map overlap may be physiologically relevant and would suggest that specificity in motor output is achieved through additional regulation and not just the topographical layout of the motor cortex. Conceivably, LBM could be extended to single neurons to address whether excitation of individual neurons[26] within overlapping map areas can evoke both forelimb and hindlimb muscle excitation, or whether individual neurons are dedicated to specific limbs. Notably, we have shown previously that reorganization after a stroke can cause individual somatosensory neurons (normally preferentially activated by signals from a single limb) to process information from multiple limbs, suggesting that single neurons can assume multiple roles[20]. With regard to sensory maps, LBM shows that the centers of sensory and motor maps are generally ~0.5–1 mm apart (**Fig. 6**), supporting lower-resolution studies using ICMS in rats that had identified these areas as a mixed sensorimotor cortex[27,28].

The resolution of LBM depends on its ability to activate subsets of cortex despite the scattering of light and despite the presence of overlapping axons and dendrites from neurons with cells bodies outside of the activation area. Estimation of the cortical area LBM activates is a complex function of light scattering and depth-dependent changes in excitability. However, we can define a lower limit based on the size of the hindlimb motor map we observed (~0.65 mm^2 or 0.9 mm in diameter). We estimated the area of cortex activated by LBM pulses using IOS imaging. The area showing > 50% of maximal activation was approximately 0.8 mm^2 (measured at full width at half-maximal amplitude), about the size of the hindlimb motor map. Notably, IOS activation profiles of point-source ICMS electrodes were also relatively large, indicating that improvements in light delivery may not lead to large gains in resolution. Given that excitation of motor neurons would not be linearly related to IOS changes and that the method does not directly read out activity within output neurons, it is possible that the spatial resolution of LBM is substantially greater than we estimated. Despite some uncertainty about map edge position, map center positions would be expected to be more precise and should accurately define the location of motor maps and potential changes after experimental manipulations. To improve the resolution of LBM, future work could use red-shifted variants of ChR2 (ref. 29) using wavelengths of light that are less susceptible to scattering in tissue. Perhaps the largest gain in resolution would be from making a transgenic rat with ChR2 expression driven by the *Thy1* promoter, where the motor cortex would be at least threefold larger[23].

Most previous motor-mapping studies have been conducted in rats or other larger species, but the variety of available transgenic mice makes them an increasingly attractive experimental model. As other strains become available, it will be interesting to conduct motor or intracortical mapping studies using mice that express ChR2 in other cortical layers or groups of neurons. LBM could also be extended to more complex movements using patterned stimulation or multisite activation[30].

METHODS

Mouse preparation, anesthesia and optical stimulation parameters. Animal protocols were approved by the University of British Columbia Animal Care Committee. Channelrhodopsin-2 transgenic mice[11] were purchased from the Jackson Labs (line 18, stock 007612, strain B6.Cg-Tg(Thy1-COP4/EYFP)18Gfng/J). After craniectomy, the mouse was fixed to the scanning stage, and the locations of its somatosensory forelimb and hindlimb representations were visualized using IOS imaging[20]. During craniectomy surgery and IOS imaging the mouse was anesthetized with isoflurane (1.5% in air). Ketamine-xylazine (100 mg kg^{-1} ketamine, 10 mg kg^{-1} xylazine) anesthetic was used during motor mapping. We generally collected several cortical EEG-based maps at the beginning of each experiment using low laser power (40 mW mm^{-2}) and short activation duration (1 ms). In some cases when responses were weak (usually when craniectomies were imperfect), we increased laser power (up to 200 mW mm^{-2}) and/or duration (up to 5 ms). We then connected the EMG electrodes and laser motion sensor, and began collecting motor maps. These EMG experiments were typically conducted using increased laser power (40–600 mW mm^{-2}) and duration (up to 35 ms), with stimulus parameters adjusted to suprathreshold levels.

Additional methods. Descriptions of surgeries, photostimulation, imaging, ICMS, EEG and EMG recording, software and data analysis are available in **Supplementary Methods**.

Note: Supplementary information is available on the Nature Methods website.

ACKNOWLEDGMENTS

This work was supported by operating grants to T.H.M. (MOP-12675) and the In Vivo Imaging Centre from the Canadian Institutes of Health Research. We thank P. Wang, H. Erb, C. Jiang, A. Tung and N. Scott for assistance.

AUTHOR CONTRIBUTIONS

O.G.S.A. and T.C.H. collected and analyzed data, and prepared the manuscript. J.D.B. developed software, analyzed data and performed histological analyses. A.G. performed optical design and fabrication of the device. T.H.M. conceived the work, analyzed data and prepared the manuscript.

COMPETING INTERESTS STATEMENT

The authors declare competing financial interests: details accompany the full-text HTML version of the paper at http://www.nature.com/naturemethods/.

Published online at http://www.nature.com/naturemethods/
Reprints and permissions information is available online at
http://npg.nature.com/reprintsandpermissions/

1. Penfield, W. & Boldrey, E. Somatic motor and sensory representation in the cerebral cortex of man as studied by electrical stimulation. *Brain. J. Neurol.* **60**, 389–443 (1937).
2. Donoghue, J.P. & Sanes, J.N. Peripheral-nerve injury in developing rats reorganizes representation pattern in motor cortex. *Proc. Natl. Acad. Sci. USA* **84**, 1123–1126 (1987).
3. Hosp, J.A. *et al.* Thin-film epidural microelectrode arrays for somatosensory and motor cortex mapping in rat. *J. Neurosci. Methods.* **172**, 255–262 (2008).
4. Siebner, H.R. & Rothwell, J. Transcranial magnetic stimulation: new insights into representational cortical plasticity. *Exp. Brain Res.* **148**, 1–16 (2003).
5. Shepherd, G.M.G., Pologruto, T.A. & Svoboda, K. Circuit analysis of experience-dependent plasticity in the developing rat barrel cortex. *Neuron* **38**, 277–289 (2003).
6. Luo, L., Callaway, E.M. & Svoboda, K. Genetic dissection of neural circuits. *Neuron* **57**, 634–660 (2008).
7. Huber, D. *et al.* Sparse optical microstimulation in barrel cortex drives learned behaviour in freely moving mice. *Nature* **451**, 61–64 (2008).
8. Zhang, F., Aravanis, A.M., Adamantidis, A., de Lecea, L. & Deisseroth, K. Circuit-breakers: optical technologies for probing neural signals and systems. *Nat. Rev. Neurosci.* **8**, 577–581 (2007).
9. Nagel, G. *et al.* Channelrhodopsins: directly light-gated cation channels. *Biochem. Soc. Trans.* **33**, 863–866 (2005).
10. Boyden, E.S., Zhang, F., Bamberg, E., Nagel, G. & Deisseroth, K. Millisecond-timescale, genetically targeted optical control of neural activity. *Nat. Neurosci.* **8**, 1263–1268 (2005).
11. Arenkiel, B.R. *et al.* In vivo light-induced activation of neural circuitry in transgenic mice expressing channelrhodopsin-2. *Neuron* **54**, 205–218 (2007).
12. Callaway, E.M. & Katz, L.C. Photostimulation using caged glutamate reveals functional circuitry in living brain-slices. *Proc. Natl. Acad. Sci. USA* **90**, 7661–7665 (1993).
13. Feng, G.P. *et al.* Imaging neuronal subsets in transgenic mice expressing multiple spectral variants of GFP. *Neuron* **28**, 41–51 (2000).
14. Aravanis, A.M. *et al.* An optical neural interface: in vivo control of rodent motor cortex with integrated fiberoptic and optogenetic technology. *J. Neural Eng.* **4**, S143–S156 (2007).
15. Rho, M.J., Lavoie, S. & Drew, T. Effects of red nucleus microstimulation on the locomotor pattern and timing in the intact cat: a comparison with the motor cortex. *J. Neurophysiol.* **81**, 2297–2315 (1999).
16. Murphy, T.H., Li, P., Betts, K. & Liu, R. Two-photon imaging of stroke onset in vivo reveals that NMDA-receptor independent ischemic depolarization is the major cause of rapid reversible damage to dendrites and spines. *J. Neurosci.* **28**, 1756–1772 (2008).
17. Ferezou, I. *et al.* Spatiotemporal dynamics of cortical sensorimotor integration in behaving mice. *Neuron* **56**, 907–923 (2007).
18. Raineteau, O. & Schwab, M.E. Plasticity of motor systems after incomplete spinal cord injury. *Nat. Rev. Neurosci.* **2**, 263–273 (2001).
19. Brown, C.E., Li, P., Boyd, J.D., Delaney, K.R. & Murphy, T.H. Extensive turnover of dendritic spines and vascular remodeling in cortical tissues recovering from stroke. *J. Neurosci.* **27**, 4101–4109 (2007).
20. Winship, I.R. & Murphy, T.H. In vivo calcium imaging reveals functional rewiring of single somatosensory neurons after stroke. *J. Neurosci.* **28**, 6592–6606 (2008).
21. Trachtenberg, J.T. *et al.* Long-term *in vivo* imaging of experience-dependent synaptic plasticity in adult cortex. *Nature* **420**, 788–794 (2002).
22. Xu, H.T., Pan, F., Yang, G. & Gan, W.B. Choice of cranial window type for *in vivo* imaging affects dendritic spine turnover in the cortex. *Nat. Neurosci.* **10**, 549–551 (2007).
23. Kleim, J.A. *et al.* Functional organization of adult motor cortex is dependent upon continued protein synthesis. *Neuron* **40**, 167–176 (2003).
24. Teskey, G.C., Monfils, M.H., VandenBerg, P.M. & Kleim, J.A. Motor map expansion following repeated cortical and limbic seizures is related to synaptic potentiation. *Cereb. Cortex.* **12**, 98–105 (2002).
25. Franklin, K.B.J. & Paxinos, G. The mouse brain. In *Stereotaxic Coordinates* (Academic Press, New York, 1997).
26. Herfst, L.J. & Brecht, M. Whisker movements evoked by stimulation of single motor neurons in the facial nucleus of the rat. *J. Neurophysiol.* **99**, 2821–2832 (2008).
27. Hall, R.D. & Lindholm, E.P. Organization of motor and somatosensory neocortex in albino rat. *Brain Res.* **66**, 23–38 (1974).
28. Sievert, C.F. & Neafsey, E.J. A chronic unit study of the sensory properties of neurons in the forelimb areas of rat sensorimotor cortex. *Brain Res.* **381**, 15–23 (1986).
29. Zhang, F. *et al.* Red-shifted optogenetic excitation: a tool for fast neural control derived from Volvox carteri. *Nat. Neurosci.* **11**, 631–633 (2008).
30. Graziano, M.S.A., Cooke, D.F., Taylor, C.S.R. & Moore, T. Distribution of hand location in monkeys during spontaneous behavior. *Exp. Brain Res.* **155**, 30–36 (2004).